Measurement of the beam polarization at the ILC using $e^+e^- \to W^+W^- \to qq\ell\nu$ data

A. Rosca[1]

[1] DESY, Hamburg, D 22607, Germany

Abstract

An assessment of the achievable precision on the measurement of the longitudinal polarization of high energy electron and positron beams in collision at the International Linear Collider operated at 1 TeV is presented. Two methods to extract the beam polarization using the $e^+e^- \to W^+W^- \to qq\ell\nu$ process are investigated: a modified Blondel scheme with both beams polarized and an angular fit method based on the W-boson production angle.

1 Introduction

The measurement of the beam polarization at the ILC will be performed by Compton polarimeters. They will measure the average beam polarization at their location with high statistics. Due to effects such as polarization spread, spin transport between the polarimeter and interaction point, and disruptions due to beam-beam effects, the result of the polarimeter measurement will differ from the luminosity-weighted beam polarization. Using a physics process that is sensitive to the beam polarization, the average luminosity-weighted polarization at the interaction point can be directly extracted. The process $e^+e^- \to W^+W^-$ can be used to achieve this goal.

We compare two techniques to measure the polarization: a modified Blondel scheme that relies on the dependence of the total cross sections of semileptonic W-pair production for different incoming beam polarizations, and an angular fit method that uses the distribution of the production angle $\cos\theta_W$ of the W^- with respect to the electron beam axis.

This study investigates the capability of the ILD detector to measure the longitudinal polarization of high energy electron and positron beams at the ILC operated at $\sqrt{s} = 1$ TeV. The simulation of the signal and background processes is described in Section 2. Event selection is described in Section 3. The methods to extract the polarization are presented in Section 4 and conclusions are summarized in Section 5. The achievable accuracy of this measurement for the ILC at $\sqrt{s} = 500$ GeV has been reported by [7].

2 Simulation of the signal and background processes

Signal and background events are generated using the WHIZARD [1] event generator. The effects of initial state radiation and beamstrahlung are included. The four- momenta of the final-state quarks and leptons are passed as input to PYTHIA 6.422 [2] for parton showering and hadronization. The detector response is simulated using the MOKKA [3] full Monte Carlo detector simulation.

The detector model used in this analysis is ILD_o1_v05 and it is described in Reference [4].

Events were generated at a centre-of-mass energy of 1 TeV assuming 100% polarized beams. Events corresponding to different polarization configurations were obtained by properly mixing the samples in order to obtain realistic cases of partial polarizations. The final results are reported for an integrated luminosity of 1000 fb^{-1}, but propagation of the uncertainties at different luminosities are also shown.

The hadronic cross-section for $\gamma\gamma \to$ hadrons events, with mass exceeding 2 GeV, is several hundred nb [5], so that about 4.1 events of this type are produced per bunch crossing. These events (pile-up) are overlaid to the physics events. Since the pile-up events are produced in the t-channel q-exchange most of the resulting final state particles are distributed at low angles.

3 Event selection

W bosons decay into hadrons, mostly through $W^- \to \bar{u}d$ or $\bar{c}s$, or leptons, $W^- \to \ell^-\bar{\nu}_\ell$, where ℓ denotes an electron, muon or tau lepton. W-boson pair production yields three classes of events: the fully- leptonic, $\ell\nu\ell\nu$, the semi-leptonic, $qq\ell\nu$, and the fully-hadronic, $qqqq$, final states. Due to the presence of more than one neutrino in the $\ell\nu\ell\nu$ final state, the masses of the W bosons cannot be directly reconstructed from their decay products and this decay channel is not further considered here. The $qqqq$ final state has been excluded as well due to the fact that the charge of the W-boson cannot be reconstructed with sufficient precision from the jets of the hadronic decay.

In order to measure the charge of the W-boson with high purity we only considered here the semi-leptonic final state $qq\ell\nu$ where ℓ denotes an electron or a muon. The channel $qq\tau\nu$ is considered as a background as well.

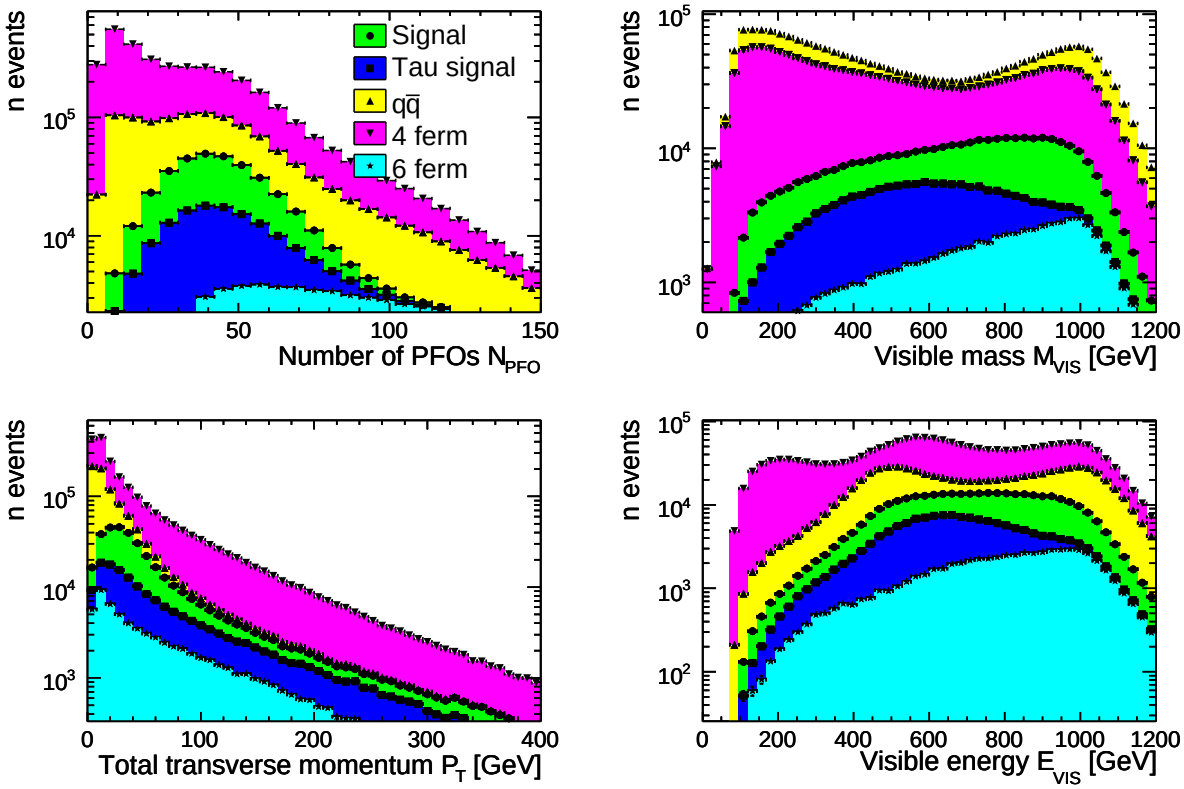

Figure 1: Distributions of the number of PFO N_{PFO} (top left), visible mass M_{VIS} (top right), total transverse momentum P_T (bottom left) and visible energy E_{VIS} (bottom right). Events with pile-up.

Visible final-state fermions are reconstructed in each event. Electrons and muons from W-boson decays are measured in the calorimeters and in the tracking system. Lepton candidates are defined by the following ratios: E_{ECAL}/E_{tot} and E_{tot}/p_{track}, where E_{ECAL} is the energy measured in the electromagnetic calorimeter, E_{tot} is the total measured energy in the calorimeters, and p_{track} is the measured track momentum in the tracking detectors. We require that E_{ECAL}/E_{tot} is greater than 0.9 for electrons and less than 0.5 for muons and E_{tot}/p_{track} be greater than 0.8 for electrons and below 0.4 for muons. Jets originating from quarks are reconstructed by combining information from calorimetric clusters and associated tracks into jets using the kt algorithm [6], see section 3.2.

The event selection for the process $qq\ell\nu$ requires high particle-multiplicity, an identified lepton, and missing momentum.

Events are selected requiring the number of reconstructed particle flow objects N_{PFO} be greater than 15, the total transverse momentum P_T larger than 5 GeV, a total visible energy below 1200 GeV and a visible mass greater than 100 GeV. The distributions of the variables used for the preselection of the $qq\ell\nu$ events are shown in Figure 1.

3.1 Identification of isolated leptons

In the $qq\ell\nu$ final state, the lepton from the $W \to \ell\nu$ tends to be energetic and isolated from the rest of the event. To identify an isolated lepton, a cone with a half-opening angle θ_{cone} is constructed around each lepton candidate. The cone energy E_{cone} is defined to be the sum of the energy of all the tracks inside the cone, excluding the lepton candidate. We require the value of the $\cos\theta_{cone}$ to be 0.98.

For illustration purposes we show in Figure 2 the distribution of the cone energy versus the lepton candidate energy for the processes $W^+W^- \to qqqq$ (in blue) and $ZZ \to \ell^+\ell^-\ell^+\ell^-$ (in red). The energetic isolated leptons have high energy and a low cone energy, thus populating the lower right

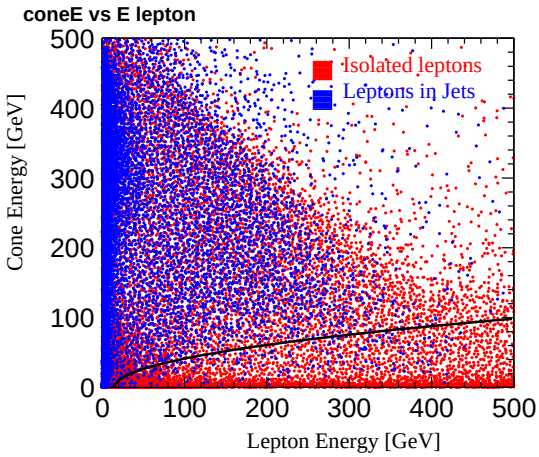

Figure 2: Distribution of the cone energy and the lepton energy. Leptons below the curve are identified as isolated leptons.

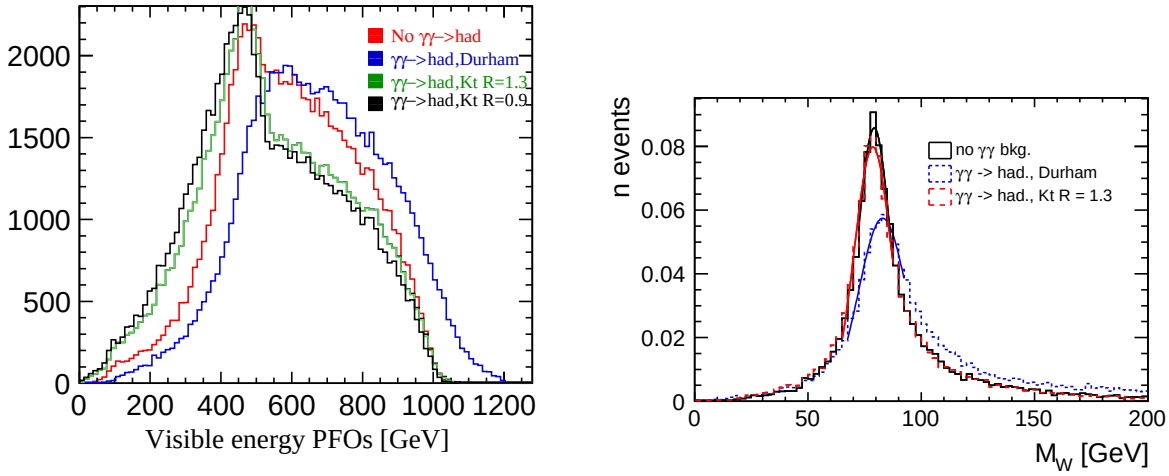

Figure 3: Left: Distribution of the visible energy of the PFOs after applying a jet clustering algorithm in events with pileup, compared to the visible energy of the PFOs in events without $\gamma\gamma$ overlay (red curve). Right: Reconstructed invariant mass of the W-boson using different jet clustering algorithms. The black curve is obtained for events without $\gamma\gamma$ overlay.

region, shown as red points in Figure 2. Leptons from heavy flavour jets are likely to be less energetic and have a higher cone energy, shown as blue dots in Figure 2. The selection of isolated leptons is performed by applying a cut on the cone energy which varies as the lepton energy and is given by the equation $E_{cone} < \sqrt{20E_\ell - 300}$. We require one and only one isolated lepton.

3.2 Jet clustering and suppression of $\gamma\gamma$ overlay events

We employ a jet clustering algorithm to separate the event into 2 jets, after taking out the isolated lepton. At the ILC, the physics event is accompanied by significant additional energy from $\gamma\gamma \rightarrow$ hadrons background. For this reason it is not possible to use the jet clustering algorithms developed for LEP which combine all particles into jets. We found that the kt algorithms [6] developed for hadron collisions are more suitable since they reduce the inclusion of background particles into the jets from the e^+e^- interaction. Figure 3 (left) compares the reconstructed visible energy observed with the Durham algorithm to that from the kt algorithm for different values of the jet radius parameter

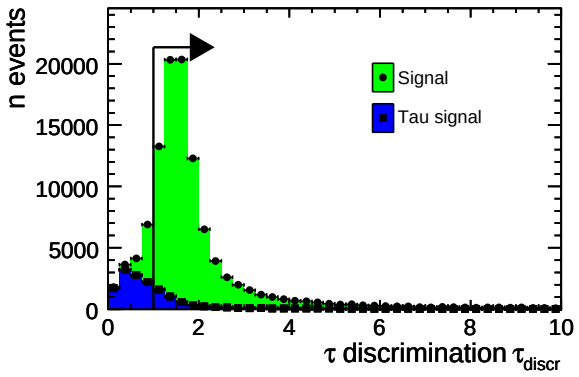

Figure 4: Distribution of the discriminating variable used to suppress tau decays of the W-boson in $qq\ell\nu$ events. The discrimination is performed requiring $\tau_{discr} > 1$.

Cut	$qq\ell\nu$	$qq\tau\nu$	2 ferm.	4 ferm.	6 ferm.
Initial events	210841.0	104698.0	776759.0	2369330.0	69277.0
Preselection	192576.7	95783.3	427708.3	1130853.3	63785.0
Single isolated lepton	117451.7	20010.0	19167.5	234110	22696.7
Fit probability	100232.0	17606.7	12490.7	68277.0	17983.3
$\tau_{discr} < 1$	91281.7	5651.0	10294.7	52409.3	16445.0
Mass cuts	76415.0	4120.0	2550.2	14051.9	3010.0
$\cos\theta_W >$ -0.95	76101.7	4100.0	2369.5	12442.5	2886.7

Table 1: Summary of the cuts to select $qq\ell\nu$ events. Estimated yields are given assuming an integrated luminosity of 100 fb^{-1} with beam polarizations (P_{e^-}, P_{e^+}) = (-0.8,+0.2).

R. The Durham algorithm adds about 100 GeV energy from the background to the reconstructed jets, while this effect is reduced using the kt algorithm.

Jets are reconstructed from PFOs using the kt algorithm in its exclusive mode with R=1.3 and using the E recombination scheme. The clustering is stopped when two jets are found.

As an example, the reconstruction of W bosons is illustrated in Figure 3 (right). The distributions obtained with and without the overlay of $\gamma\gamma$ events are compared.

3.3 Kinematic fit

A kinematic fit, assuming four-momentum conservation and other constraints, is used to improve energy and angle resolutions. The four-momentum conservation requirement determines in the case of our final state the momentum and the direction of the neutrino. The mass resolution of the two W bosons is improved by the additional constraint of requiring these masses to be equal. This procedure results in a two-constraint (2C) fit of $qq\ell\nu$ events. The reconstructed mass obtained in the 2C fit, M_{2C} fit is required to be $40 < M_{2C} < 120$ GeV.

The suppression of the $qq\tau\nu$ is performed using the same discriminating variable τ_{disc} as defined in ref. [7]. Candidates with $\tau_{disc} < 1$ are considered $qq\tau\nu$ events and rejected. Figure 4 shows the distribution of this discriminating variable.

We summarize the yields after applying each cut for the case of polarized beams (P_{e^-}, P_{e^+}) =(-0.8,+0.2) in Table 1, where the yields are normalized assuming an integrated luminosity of 100 fb^{-1}.

The total signal efficiency is estimated to be 36% in the presence of the pile-up events. The purity of the selection is 82% at 1 TeV. The residual background, not originating from W-boson pair

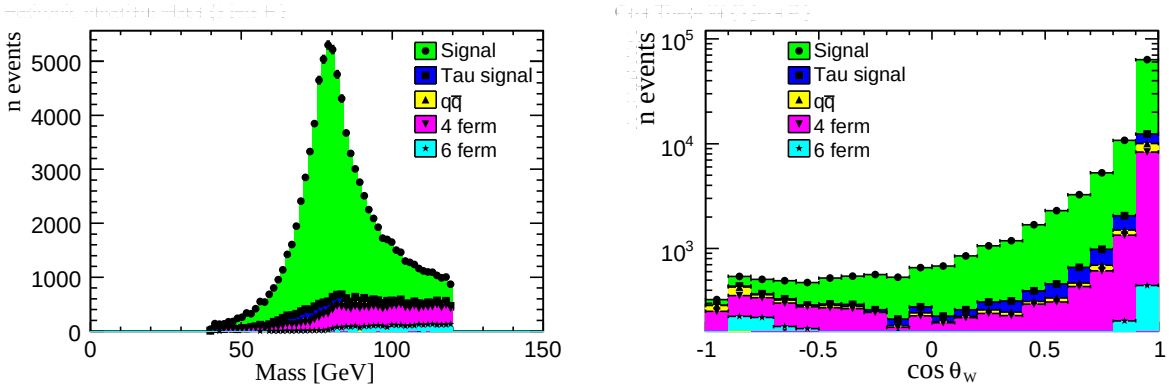

Figure 5: Left: Distribution of reconstructed W-boson mass after applying the kinematic fit using the equal-mass constraint and all selection cuts. Right: Distribution of the cosine of the polar angle of the W^-.

production, is dominated by $qqe\nu$ events (70.3%), followed by $q\bar{q}$ events (13.4%) and 6 fermion events (16.3%). The $qq\tau\nu$ events amount to 5%. The $qqe\nu$ events considered here as a background originate from single-W production and fail the signal definition:

$$M_{qq/e\nu} = M_{W^+W^-} \pm 50\ GeV.$$

The distributions of M_{2C} and $\cos\theta_W$, after applying all the cuts, are shown in Figure 5.

4 Methods to extract the beam polarization

The first method considered to measure the beam polarization is a modified Blondel scheme. This technique requires to spend some luminosity with all four possible combinations of the beam polarizations: $++$, $+-$, $-+$ and $--$, where the signs are for the positron, and respectively electron polarizations. The absolute polarization values of the left- and right-handed degrees of polarization are required to be equal. The beam polarization is obtained by measuring the total cross section for each helicity combination [8]:

$$|P_{e^\pm}| = \sqrt{\frac{(\sigma_{-+} + \sigma_{+-} - \sigma_{--} - \sigma_{++})(\pm\sigma_{-+} \mp \sigma_{+-} + \sigma_{--} - \sigma_{++})}{(\sigma_{-+} + \sigma_{+-} + \sigma_{--} + \sigma_{++})(\pm\sigma_{-+} \mp \sigma_{+-} - \sigma_{--} + \sigma_{++})}},$$

where σ_{+-} is the total cross section measured for right-handed positron beam and left-handed electron beam (σ_{--} and σ_{++} are defined analogously) and P_{e^+} (P_{e^-}) is the resulting positron (electron) beam polarization.

The four cross sections σ_{++}, σ_{+-}, σ_{-+} and σ_{--} have been measured using Monte Carlo samples for an integrated luminosity of 100 fb^{-1}. The equation above has been applied and the statistical uncertainty on the measured polarizations has been calculated. The error has been propagated towards higher luminosities, as shown in Figure 6 (left). The total luminosity is assumed to be shared equally between the four polarization sets. For a total integrated luminosity of 1000 fb^{-1} the precision obtained on the electron and positron polarizations is $\Delta P_{e^-}/P_{e^-} = 0.44\%$ and $\Delta P_{e^+}/P_{e^+} = 1.19\%$, respectively.

The Blondel scheme requires high integrated luminosities in order to obtain small uncertainties on the polarization. This motivates the use of alternative techniques, for instance an angular fit to the $\cos\theta_W$-distribution. This method uses the additional information contained in the distribution of the W-pair production angle.

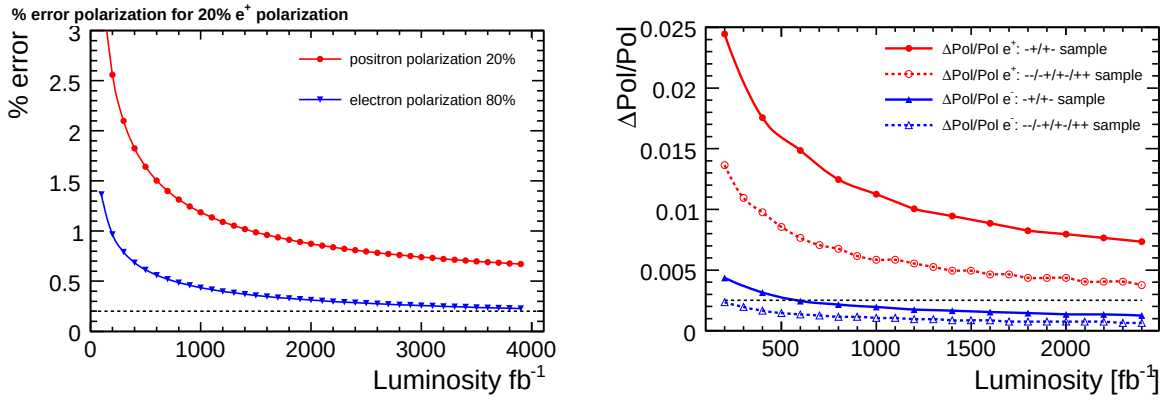

Figure 6: Statistical precision on the polarization obtained with the Blondel technique (left). The integrated luminosity is shared equally between the four polarization sets. Results for the angular fit method are also shown (right). Here the integrated luminosity is divided equally between $\mathcal{P}_{-80,+20}$ and $\mathcal{P}_{+80,-20}$ (solid lines) or it is divided among $\mathcal{P}_{-80,-20}$, $\mathcal{P}_{-80,+20}$, $\mathcal{P}_{+80,-20}$ and $\mathcal{P}_{+80,+20}$ in the proportions 1:4:4:1 (dotted lines). The horizontal dashed line indicates the optimum precision of 0.2%.

The angular fit method is based on the creation of Monte Carlo templates of the $\cos\theta_W$ distribution for several sets of beam polarizations. The electron (positron) polarization was scanned in the interval [-90%,+90%] ([-70%,+70%]). Each distribution is divided into 20 bins, which cover the full range of variability of $\cos\theta_W$ [-0.95,+1]. The $\cos\theta_W$ distribution of the data are fitted to the templates in order to measure the polarization using MINUIT [9]. The fit has been performed with two free parameters for P_{e^-} and P_{e^+}, with a linear least squares minimization:

$$\chi^2 = \sum_{j=1}^{4}\sum_{i=1}^{20} \frac{(N_{i,j}^{DATA} - f_i(\pm P_{e^+}, \pm P_{e^-}))^2}{N_{i,j}^{DATA}},$$

where $N_{i,j}^{DATA}$ is the content of the i-th bin of the $\cos\theta_W$ distribution for the j-th data sample of the four samples for different helicity sets. The Monte Carlo template f_i for the same bin of $\cos\theta_W$ and the polarizations P_{e^-} and P_{e^+} depend on the sample j. For each considered integrated luminosity the fit is repeated several times. The resulting fit parameters are Gaussian distributed around the expected value, as shown in Figure 7. The fit statistical errors are obtained from the widths of the Gaussian fitted to the parameter distributions.

The precision achieved with the angular fit method is summarized in Figure 6 (right).

The angular fit is more powerful than the Blondel technique, yielding the same precisions at much lower luminosities. For an integrated luminosity of 1000 fb^{-1} divided among the four polarization sets $\mathcal{P}_{-80,-20}$, $\mathcal{P}_{-80,+20}$, $\mathcal{P}_{+80,-20}$ and $\mathcal{P}_{+80,+20}$ in the proportion 1:4:4:1 the precision obtained on the electron and positron polarizations is $\Delta P_{e^-}/P_{e^-} = 0.11\%$ and $\Delta P_{e^+}/P_{e^+} = 0.6\%$, respectively.

We also assessed the achievable error on the polarizations when reducing to zero the integrated luminosity spent on the $++$ and $--$ polarization sets. Such configurations of the helicities are of low interest for most of the physics studies, since they suppress the s-channel production. The results obtained are shown in Figure 6 (right, solid lines). For an integrated luminosity of 1000 fb^{-1} the precision obtained on the electron and positron polarizations is $\Delta P_{e^-}/P_{e^-} = 0.19\%$ and $\Delta P_{e^+}/P_{e^+} = 1.13\%$, respectively.

5 Conclusions

Using W-pair production it will be possible to measure the average luminosity-weighted beam polarization at the ILC with high sensitivity. Assuming an integrated luminosity of 1000 fb^{-1} at $\sqrt{s}$=1

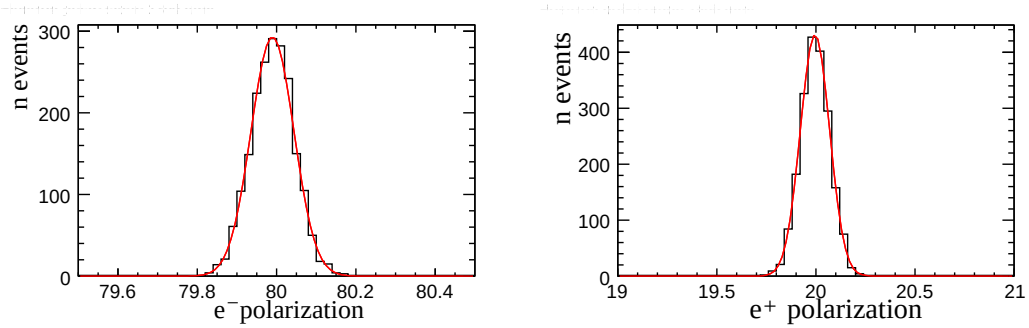

Figure 7: Distributions of the fitted parameters for the electron (left) and positron (right) polarizations.

	ΔP_{e^-}	$\Delta P_{e^-}/P_{e^-}$	ΔP_{e^+}	$\Delta P_{e^+}/P_{e^+}$
Blondel technique (25% ++/+−/−+/−−)	0.0035	0.44%	0.0024	1.19%
Fit method (10% ++/−−) (40% +−/−+)	0.00084	0.11%	0.0012	0.6%
Fit method (50% +−/−+)	0.0016	0.19%	0.0023	1.13%

Table 2: Achievable errors for the two beam polarizations using $qq\ell\nu$ events and 1000 fb^{-1} at $\sqrt{s}$ = 1 TeV.

TeV, Table 2 summarizes the obtainable errors on the electron and positron polarizations.

The study has not yet evaluated all backgrounds, particularly $\gamma\gamma$ and $e\gamma$ processes need to be looked at in more detailed. If the impact of these backgrounds becomes important, the selection cuts can be tightened with an expected degradation of the efficiency by a factor about 1.8.

Also it should be mentioned that the precision of the angular fit method does not depend on assuming that the TGCs are consistent with the SM expectations. A simultaneous fit of the polarization and TGCs is possible [7] without loosing sensitivity on the polarization.

References

[1] W. Kilian, T. Ohl, and J. Reuter, "WHIZARD: Simulating multi-particle processes at LHC and ILC", Eur.Phys.J. **C71** (2011) 1742, arXiv:0708.4233 [hep-ph].

[2] T. Sjoestrand, S. Mrenna, and P. Skands, J. High Energy Phys. 05 (2006) 026.

[3] P. Mora de Freitas and H. Videau, "Detector simulation with MOKKA/Geant4: Present and future", LC-TOOL-2003-010;
http://polzope.in2p3.fr:8081/MOKKA.

[4] T. Abe et al. [ILD Concept Group - Linear Collider Collaboration], "The International Large Detector: Letter of Intent", KEK Report 2009-06

[5] The Particle Data Group, K. Hagiwara et al., Phys. Rev. **D66** (2002) 010001.

[6] M. Cacciari, G.P. Salam, *Dispelling the N3 myth for the kt jet-finder* Phys. Lett.B 641 (2006) 57

[7] I. Marchesini, "Triple gauge couplings and polarization at the ILC and leakage in a highly granular calorimeter", DESY-THESIS-2011-044.
P. Bechtle, W. Ehrenfeld and I. Marchesini, "Triple gauge couplings and polarization at the ILC", LC-DET-2009-003.

[8] K. Moenig, "The use of positron polarization for precision measurements", LC-PHSM-2000-059.

[9] F. James and M. Roos, "Minuit: A system for function minimization and analysis of the parameter errors and correlations", Comput. Phys. Commun., 10:343-367, 1975.

Acknowledgments

The author would like to thank I. Marchesini and the members of the ILD physics working group for many helpful discussions, as well as the generation and production teams.